

Understanding mechanisms of thermal expansion in PbTiO_3 thin-films from first principles: role of high-order phonon-strain anharmonicity

Ethan T. Ritz

*Sibley School of Mechanical and Aerospace Engineering,
Cornell University, Ithaca, New York 14853, USA*

Nicole A. Benedek*

*Department of Materials Science and Engineering,
Cornell University, Ithaca, New York 14853, USA*

(Dated: March 24, 2021)

The thermal properties of materials are critically important to various technologies and are increasingly the target of materials design efforts. However, it is only relatively recent advances in first-principles computational techniques that have enabled researchers to explore the microscopic mechanisms of thermal properties, such as thermal expansion. We use the Grüneisen theory of thermal expansion in combination with density functional calculations and the quasiharmonic approximation to uncover mechanisms of thermal expansion in PbTiO_3 thin-films in terms of elastic and vibrational contributions to the free energy. Surprisingly, we find that although the structural parameters of PbTiO_3 thin-films evolve with temperature as if they are dominated by linear elasticity, PbTiO_3 thin-films are strongly anharmonic, with large changes in the elastic constants and Grüneisen parameters with both misfit strain and temperature. We show that a fortuitous near-cancellation between different types of anharmonicity gives rise to this behavior. Our results illustrate the importance of high-order phonon-strain anharmonicity in determining the temperature-dependent structural parameters of PbTiO_3 thin-films, and highlight the complex manner in which thermal expansion, misfit strain and elastic and vibrational properties are intertwined.

I. INTRODUCTION

Recent advances in theoretical and experimental techniques have promoted increasing interest in the phonon and thermal properties of materials by making it possible to more easily access the information required to elucidate atomic-scale mechanisms.[1–4] Particularly exciting progress has been made in the family of metal-organic frameworks, where it now not only appears possible to design materials with unconventional thermal responses (such as negative thermal expansion), but also to tune those responses in a highly controllable way [5–7]. In contrast, negative thermal expansion is both rarer and apparently more difficult to tune in inorganic framework materials, such as complex oxides [8–10]. The most common approach is chemical substitution, although it is generally challenging to change either the sign or the magnitude of the thermal expansion significantly in this way (recent work provides an impressive exception [11, 12]). A significant barrier to designing effective strategies for highly tunable thermal expansion is that, with few exceptions, the microscopic factors controlling the temperature evolution of structural parameters are poorly understood.

The ferroelectric $P4mm$ tetragonal phase of PbTiO_3 exhibits negative volumetric thermal expansion from approximately room temperature up to 760 K, where it undergoes a structural phase transition to a cubic $Pm\bar{3}m$

phase [13, 14]. Thermal expansion in the ferroelectric phase is characterized by a shrinking c -axis and an expanding a -axis – the c -axis contracts faster than the a -axis expands, so the net effect is a decrease in volume with increasing temperature. Interestingly, recent theoretical work has shown that negative thermal expansion in PbTiO_3 is actually *driven* by the expanding a -axis [4]. However, strong elastic (Poisson-like) coupling between the a - and c -axes pulls the c -axis down as the a -axis expands.

It is possible to grow high-quality thin-films of PbTiO_3 on various substrates, and a wealth of temperature-dependent structural and ferroelectric polarization data are available in the literature. Thin-film systems are excellent platforms for probing mechanisms of thermal expansion because different substrates will impart different misfit strains (which will change with temperature, depending on the thermal expansion coefficient of the substrate[15, 16]) and hence different elastic boundary conditions to the growing film. Hence, it becomes possible to understand how changes in the unit cell dimensions affect thermal expansion behavior, all while keeping the chemical composition constant.

In previous work, we used first-principles density functional theory (DFT) and the quasiharmonic approximation (QHA) to investigate the thermal expansion of PbTiO_3 thin-films on SrTiO_3 , DyScO_3 and $(\text{La}_{0.29(5)}\text{Sr}_{0.71(5)})_{\text{A-site}}(\text{Al}_{0.65(1)}\text{Ta}_{0.35(1)})_{\text{B-site}}\text{O}_3$ (LSAT) substrates. Our key findings were that: 1) the misfit strain does not just change the properties of PbTiO_3 thin-films, it changes how they change with temperature, and 2) the mismatch in thermal expansion co-

* nbenedek@cornell.edu

efficients between PbTiO_3 and the substrates had a striking effect on thin-film properties. For a given misfit strain, we found qualitative changes in thermal expansion behavior and ferroelectric transition temperatures depending on the thermal expansion coefficient of the substrate.

In this work, we use the Grüneisen theory of thermal expansion in combination with DFT calculations and the quasiharmonic approximation to elucidate the microscopic mechanisms underlying the structural properties of PbTiO_3 thin-films in terms of elastic and vibrational contributions to the lattice parameters at finite temperatures. Surprisingly, we show that the c -axis lattice parameter (perpendicular to the substrate) evolves with temperature as if it is almost entirely dominated by linear elastic effects, despite the fact that PbTiO_3 thin-films exhibit the hallmarks of strong anharmonicity. We find that this behavior is due to a fortuitous near-cancellation between the contributions to thermal expansion from anharmonic elasticity and from vibrational thermal stress, the details of which depend both on the mismatch between the lattice parameters of the film and substrate, as well as the mismatch between their rates of thermal expansion. We use our findings to explain the temperature evolution of the structural, elastic, vibrational and thermal expansion properties of PbTiO_3 thin-films on experimentally available substrates.

II. FIRST-PRINCIPLES CALCULATIONS

All calculations were performed using density functional theory, as implemented in Quantum Espresso 6.5.0. [17] We used the Wu-Cohen exchange-correlation functional [18] with Garrity-Bennett-Rabe-Vanderbilt ultrasoft pseudopotentials.[19] The following states were included in the valence for each element: $5d^{10}6s^26p^2$ for Pb, $3s^23p^64s^23d^1$ for Ti, and $2s^22p^4$ for O. Zero temperature unit cell lattice parameters and atomic positions of $P4mm$ PbTiO_3 were converged with respect to the plane wave cutoff energy and \mathbf{k} -point mesh density to within 0.001 Å. Unless otherwise mentioned, structural parameters were found to be converged at a force cutoff threshold of 3.0×10^{-5} Ry/bohr using a $6 \times 6 \times 6$ Monkhorst-Pack (MP) mesh and a 100 Ry plane wave cutoff energy, compared with MP meshes up to $12 \times 12 \times 12$ and plane wave cutoffs up to 120 Ry. Phonon dispersion calculations were performed using density functional perturbation theory on an $8 \times 8 \times 8$ \mathbf{q} -point grid.

Finite temperature structural parameters and elastic constants were predicted using a quasiharmonic approximation (QHA) to the Helmholtz free energy – in this study, we closely follow the framework outlined in Refs. 20 and 21 regarding the application of the QHA. Our grid of strained systems consisted of a 6×12 grid spanning -1.5 to +2.5% strain along the a -axis of the $P4mm$ tetragonal phase, and -4.0% to +5.1% strain along c , augmented with 20 additional points with strains spanning

-1.1% to -0.3% strain in a and -4.0% to +5.1% strain in c . These points were chosen to ensure good convergence of finite-temperature elastic constants and to make sure that for bulk PbTiO_3 and all strained films studied, the lattice parameters as a function of temperature would be bounded by these values [22]. Some structures at very large values of strain exhibited phonons with imaginary frequencies; these points were discarded from the data set. Note that the strain values above are defined with respect to the 0 K lattice parameters of the $P4mm$ phase, including zero-point energy corrections from vibrational degrees of freedom (we find $a = 3.891$ Å and $c = 4.174$ Å).

We use the same definitions of misfit strain and thermal expansion mismatch as in Ref. 21; we reproduce the definitions here for convenience. For the calculations of epitaxially strained PbTiO_3 , we clamp the in-plane (a and b) lattice parameters of PbTiO_3 to the temperature-dependent lattice parameters of the substrate. That is, our misfit strain is defined as,

$$\varepsilon_a(T) = \frac{a_{\text{substrate}}(T) - a_{\text{PTO}}(T)}{a_{\text{PTO}}(T)}, \quad (1)$$

where $a_{\text{substrate}}(T)$ is the lattice parameter of the substrate at some temperature T , and $a_{\text{PTO}}(T)$ is the in-plane lattice parameter of bulk PbTiO_3 at the same temperature from our QHA calculations. We can re-write this (as in Ref. 21) as

$$\varepsilon_a(T) = \varepsilon_a^{300} + \varepsilon_a^{\text{thermal}}(T), \quad (2)$$

where ε_a^{300} is the strain at a reference temperature of 300 K (the misfit strain is usually defined at room temperature in the thin-film literature by convention), and the additional strain that arises from changes in temperature $\varepsilon_a^{\text{thermal}}$ is defined as

$$\begin{aligned} \varepsilon_a^{\text{thermal}}(T) &= \int_{\tau=300}^T \alpha_a(\tau) - \alpha_a^{\text{bulk}}(\tau) d\tau \\ &= \int_{\tau=300}^T \Delta\alpha_a(\tau) d\tau, \end{aligned} \quad (3)$$

The misfit strain rate is defined as $\Delta\alpha_a(T) = \alpha_a(T) - \alpha_a^{\text{bulk}}(T)$, where $\alpha_a(T)$ is the thermal expansion coefficient of the substrate, and $\alpha_a^{\text{bulk}}(T)$ is the rate of thermal expansion along a for unconstrained bulk PbTiO_3 (since we are considering PbTiO_3 films coherently clamped to the substrate, the thermal expansion coefficient of PbTiO_3 films along the a -axis is just that of the substrate).

III. GRÜNEISEN THEORY OF THERMAL EXPANSION

In our previous work[21] on thermal expansion in ferroelectric PbTiO_3 thin-films, we showed that the temperature of the transition (T_c) to the cubic $Pm\bar{3}m$ phase

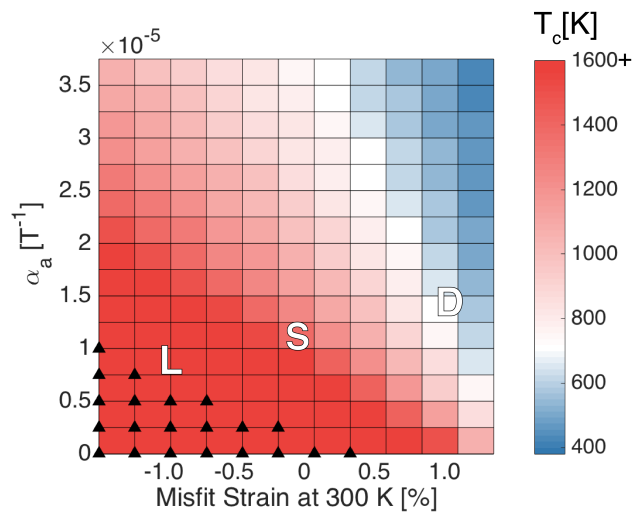


FIG. 1. Variation in ferroelectric transition temperature and c -axis behavior of ferroelectric PbTiO_3 thin-films as a function of misfit strain and substrate coefficient of thermal expansion (α_a) from our first-principles QHA calculations reported in Ref. 21. The color chart for T_c has white set to the bulk PbTiO_3 transition temperature of 760 K. Blue (red) squares indicate a strain and α_a combination that produces films with a lower (higher) T_c than bulk. Triangles indicate combinations of strain and α_a that produce films in which the c -axis continues to grow with temperature and T_c is suppressed. All other combinations of strain and α_a produce films in which the c -axis shrinks with temperature and T_c is finite. Note that the films with the highest transition temperatures may exceed 1600 K or even be completely suppressed. The letters ‘L’, ‘S’ and ‘D’ denote the strain and α_a conditions corresponding to growth on LSAT, SrTiO_3 and DyScO_3 substrates. See Ref. 21 for further details.

depends *qualitatively* not only on the misfit strain but also on the thermal expansion coefficient of the substrate (α_a). For example, Figure 1 (reproduced from Ref. 21) shows that for a tensile misfit strain of 1% at 300 K, corresponding approximately to growth of PbTiO_3 on the substrate DyScO_3 , T_c can be either higher or lower than bulk PbTiO_3 , depending on the value of α_a .

There is an intimate and complex connection between the transition temperature, the misfit strain, the thermal expansion coefficient of the substrate, and the thermal expansion coefficient of the out-of-plane c -axis (α_c) of the PbTiO_3 thin-film. Rather than continuing to focus on transition temperatures, in this work we shift our attention to the fundamental relationship between the misfit strain, α_c and the thermal expansion coefficient of the substrate. Our goal is to elucidate the microscopic origins of this relationship in terms of the elastic and vibrational properties of PbTiO_3 thin-films. That is, we aim to answer the question, how can we understand differences in the thermal expansion properties of PbTiO_3 thin-films compared to bulk in terms of fundamental elasticity and vibrational properties?

A. The thermal expansion and Grüneisen tensors

We begin by describing the thermodynamic framework through which we will explore and answer the question posed above. In the Grüneisen theory of thermal expansion [23, 24], the thermal expansion can be related to a thermal stress proportional to the mean (or bulk) Grüneisen parameters. The generalized mode Grüneisen parameter [23] for phonon mode s at wave vector \mathbf{q} is defined as the change in phonon frequency ω with respect to an infinitesimal strain ϵ along Cartesian directions i and j :

$$\gamma_{s,\mathbf{q}}^{ij} \equiv -\frac{1}{\omega_{s,\mathbf{q}}} \frac{\partial \omega_{s,\mathbf{q}}}{\partial \epsilon_{ij}}. \quad (4)$$

The mean Grüneisen parameter [25, 26] is then essentially the sum of the individual mode Grüneisen parameters weighted by their specific heats, $c_{s,\mathbf{q}}$:

$$\gamma^{ij} \equiv \frac{\sum_{s,\mathbf{q}} \gamma_{s,\mathbf{q}}^{ij} c_{s,\mathbf{q}}}{\sum_{s,\mathbf{q}} c_{s,\mathbf{q}}}. \quad (5)$$

At a given temperature, the mean Grüneisen tensor can be related to the thermal strain tensor, α_j , through the elastic stiffness tensor C_{ij} , [23, 27]

$$\sum_j C_{ij} \alpha_j = \frac{C_\eta}{V} \gamma^i, \quad (6)$$

where C_η is the bulk heat capacity at constant configuration, V is the equilibrium volume and γ^i is the mean Grüneisen parameter of Equation 5 in Voigt notation. Both α_j and γ^i are 6×1 vectors and C_{ij} is a 6×6 tensor, again employing Voigt notation. We emphasize that all of the materials properties in Equation 6 are temperature dependent, including the elastic constants.

Since thermal strains are forbidden by symmetry to induce shear strains in tetragonal systems, for this work we only need to consider the upper left 3×3 block of the thermal expansion tensor. Hence, the thermal expansion tensor can be written as a 3×1 vector where the first two indices correspond to the strain per degree Kelvin of the in-plane a and b lattice parameters (necessarily equal in a tetragonal system), and the third index corresponds to strain per degree Kelvin of the out-of-plane c lattice parameter:

$$\alpha_j = \begin{bmatrix} \alpha_a \\ \alpha_a \\ \alpha_c \end{bmatrix}. \quad (7)$$

The mean Grüneisen tensor can similarly be represented as a 3×1 vector where the first two indices correspond to the mean Grüneisen parameter with respect to a and b (again, necessarily equal by symmetry) and the third index corresponds to the mean Grüneisen parameter with

respect to c :

$$\gamma^i = \begin{bmatrix} \gamma^a \\ \gamma^a \\ \gamma^c \end{bmatrix}. \quad (8)$$

These relations help us understand how changes in the mechanical boundary conditions applied to PbTiO_3 affect its vibrational properties, and in this study allow us to quantify changes in the thermal expansion properties of the PbTiO_3 film as a function of misfit strain and substrate thermal expansion coefficient.

We compute the materials properties discussed above using the results from the QHA. For α_j , we compute a numerical derivative of strain at each value of T using the predicted lattice parameters and a central finite difference method. The C_{ij} relevant to the Grüneisen framework of thermal expansion are calculated using derivatives of the Helmholtz free energy surface fit to the points in the quasi-harmonic grid with respect to strain along the a and c axes (see Supplementary Information for details). Note that since the films are under a nonzero state of in-plane strain, the elastic stiffness tensor is no longer symmetric, *i.e.* $C_{13} \neq C_{31}$, and requires both second derivatives of energy with respect to strain as well as first derivatives (stress) to calculate [28–30].

After the α_j and C_{ij} are calculated, the Grüneisen parameters can be found by solving the system of linear equations described by Equation 6. In this study, we are often only concerned with analyzing thermal expansion along c , as α_a is defined by the substrate. Thus, the only Grüneisen parameter necessary is γ_c , which can be solved for using the following relation derived from 6:

$$2C_{31}\alpha_a + C_{33}\alpha_c = \frac{C_\eta}{V}\gamma^c. \quad (9)$$

B. Relationship between linear elastic and anharmonic effects in the Grüneisen theory

Having established some basic definitions, what we would now like is an expression that relates changes (compared to bulk) in the thermal expansion properties of PbTiO_3 thin-films to corresponding changes in the elastic constants and vibrational properties (Grüneisen parameters). Let $\Delta\alpha_i(T) \equiv \alpha_i(T) - \alpha_i^{\text{bulk}}(T)$ such that $\alpha_i^{\text{bulk}}(T) + \Delta\alpha_i(T) = \alpha_i(T)$. Similarly, let $\Delta C_{ij}(T) \equiv C_{ij}(T) - C_{ij}^{\text{bulk}}(T)$, where $C_{ij}(T)$ is the temperature-dependent elastic stiffness tensor of the PbTiO_3 thin-film and $C_{ij}^{\text{bulk}}(T)$ is the elastic stiffness tensor of bulk PbTiO_3 . Finally, let $\Delta\gamma_i(T) \equiv \gamma_i(T) - \gamma_i^{\text{bulk}}(T)$, where $\gamma_i(T)$ is the i^{th} element of the Grüneisen tensor for a PbTiO_3 thin-film and $\gamma_i^{\text{bulk}}(T)$ is the Grüneisen tensor of bulk PbTiO_3 . Thus, $\Delta\alpha_i(T)$, $\Delta C_{ij}(T)$, and $\Delta\gamma_i(T)$ respectively denote the difference in thermal expansion, elastic properties, and Grüneisen parameters in the strained film from that of bulk PbTiO_3 at the same temperature.

In the Grüneisen theory of thermal expansion, the difference in thermal expansion between a PbTiO_3 film and bulk PbTiO_3 , $\Delta\alpha(T)$, is entirely accounted for by the departure of the Grüneisen parameters and elastic constants from the values they would have in the bulk system (with higher-order phonon-phonon coupling terms ignored [23, 24]). Thus, using Equation 6, for the strained film

$$\sum_j C_{ij}(T) \alpha_j(T) = \frac{C_\eta(T)}{V(T)} \gamma_i(T), \quad (10)$$

and therefore,

$$\sum_j (C_{ij}^{\text{bulk}}(T) + \Delta C_{ij}(T)) (\alpha_j^{\text{bulk}}(T) + \Delta\alpha_j(T)) = \frac{C_\eta(T)}{V(T)} (\gamma_i^{\text{bulk}}(T) + \Delta\gamma_i(T)). \quad (11)$$

Expanding Equation 11 for $i = 3$ for a tetragonal system and subtracting from it the relation in Equation 6 for the bulk system,

$$2C_{31}^{\text{bulk}}\Delta\alpha_a + C_{33}^{\text{bulk}}\Delta\alpha_c + 2\Delta C_{31}\alpha_a^{\text{bulk}} + \Delta C_{33}\alpha_c^{\text{bulk}} + 2\Delta C_{31}\Delta\alpha_a + \Delta C_{33}\Delta\alpha_c = \frac{C_\eta}{V}\Delta\gamma^c. \quad (12)$$

We remind the reader again that since the film is under non-zero stress along the a -axis, the elasticity tensor is no longer necessarily symmetric, and thus $C_{31} \neq C_{13}$. For notational simplicity, we have also dropped the (T) from each of these quantities, though they all remain functions of temperature. Solving Equation 12 for $\Delta\alpha_c$ and rearranging (see Supplementary Information for a more detailed derivation of Equations 11–13), we obtain,

$$\begin{aligned} \Delta\alpha_c = & -2\frac{C_{31}^{\text{bulk}}}{C_{33}^{\text{bulk}}}\Delta\alpha_a + \\ & \left[\left(2\frac{C_{31}^{\text{bulk}}}{C_{33}^{\text{bulk}}}\Delta\alpha_a - \alpha_c^{\text{bulk}} \right) \frac{\Delta C_{33}}{(C_{33}^{\text{bulk}} + \Delta C_{33})} \right. \\ & \left. - 2(\alpha_a^{\text{bulk}} + \Delta\alpha_a) \frac{\Delta C_{31}}{(C_{33}^{\text{bulk}} + \Delta C_{33})} \right] + \\ & \frac{C_\eta\Delta\gamma^c}{V(C_{33}^{\text{bulk}} + \Delta C_{33})}. \end{aligned} \quad (13)$$

Though it appears complex, Equation 13 establishes the sought after connection between $\Delta\alpha_c$, the *deviation* of α_c of the strained film from that of bulk PbTiO_3 , and the elastic and vibrational properties of strained PbTiO_3 films and how *they* depart from that of bulk PbTiO_3 . By understanding the physical meaning of each term in Equation 13, we can explain the microscopic mechanism underlying $\Delta\alpha_c$ in strained film systems in terms of changes in elasticity and vibrational properties:

1. We refer to the first term, $-2\frac{C_{31}^{\text{bulk}}}{C_{33}^{\text{bulk}}}\Delta\alpha_a$, as *linear elastic coupling*. This is the elastic coupling between in-plane (a -axis) and out-of-plane (c -axis) thermal strain from linear elasticity. It accounts for the change in the rate of thermal expansion along c of the film that would be predicted if the materials properties C_{ij} and γ^c did not change at all with strain.
2. We refer to the second and third terms (grouped by square brackets in Equation 13) as *elastic anharmonicity*. These terms capture how changes in the elastic properties in the strained film affect $\Delta\alpha_c$.
3. We refer to the last term, $-\frac{C_\eta\Delta\gamma^c}{V(C_{33}^{\text{bulk}}+\Delta C_{33})}$, as *anharmonic thermal stress*. This term captures how changes in phonon anharmonicity (due to phonon-strain coupling), and the thermal stress it induces in the strained film, affect $\Delta\alpha_c$.

It is clear that the difference in the c -axis thermal expansion of strained PbTiO_3 thin-films compared to bulk arises from three sources – the mismatch between the thermal expansion coefficients of the substrate and bulk PbTiO_3 ($\Delta\alpha_a$), the difference between the elastic constants of the strained film compared to those of bulk PbTiO_3 (ΔC_{31} and ΔC_{33}), and the difference between the Grüneisen parameters along the c -axis of the strained film compared to those of bulk PbTiO_3 ($\Delta\gamma_c$). Note that the misfit strain at a given temperature gives rise to changes in the elastic constants and the Grüneisen parameters ($\Delta\gamma^c$, ΔC_{31} and ΔC_{33}) at that temperature, whereas $\Delta\alpha_a$ determines the misfit strain *rate*. In the following section, we consider how each of ΔC_{31} , ΔC_{33} , $\Delta\gamma^c$, and $\Delta\alpha_a$ affect the thermal expansion of strained PbTiO_3 thin-films along the c -axis, and how they depend on misfit strain and the thermal expansion coefficient of a given substrate.

IV. RESULTS

A. Thermal expansion in strained thin-films – Importance of anharmonicity

Figure 2 shows the rate of thermal expansion along the c -axis for PbTiO_3 thin-films as a function of strain and two different substrate thermal expansions compared with bulk PbTiO_3 . When $\alpha_a = 1 \times 10^{-5}$, the negative thermal expansion along c is suppressed compared to bulk for each of the strained films. When the rate of thermal expansion of the substrate is increased ($\alpha_a = 2.5 \times 10^{-5}$), the strained films initially show an enhanced rate of negative thermal expansion along c compared to bulk, up to about 400 K. Above this temperature, bulk PbTiO_3 once again shows the largest rate of negative thermal expansion along c . The behavior of the lattice-matched films (zero misfit strain at 300 K) is always

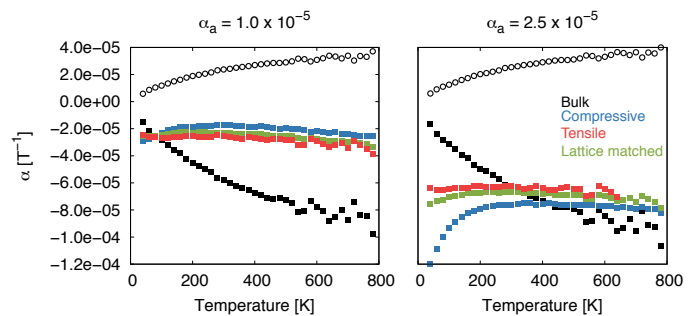


FIG. 2. Comparison between c -axis thermal expansion coefficients (α_c) as a function of temperature for bulk PbTiO_3 and a series of strained films from our QHA calculations for growth on two different substrates with $\alpha_a = 1.0 \times 10^{-5}$ (left) and 2.5×10^{-5} (right) – compressive ($\epsilon_a^{300} = -0.75\%$, tensile ($\epsilon_a^{300} = +0.75\%$) and lattice-matched ($\epsilon_a^{300} = 0.00\%$). The α_c data are denoted by closed squares, whereas the α_a data (shown for bulk PbTiO_3 only) are denoted by open black circles. The data for bulk PbTiO_3 are identical in both panels.

‘between’ that of the tensile and compressively strained films. In order to prevent the discussion below from becoming overly complex, we do not explicitly discuss the lattice-matched films.[31]

We can understand the trends shown in Figure 2 by considering individually the contributions of elastic anharmonicity, thermal stress and linear elasticity in Equation 13 to $\Delta\alpha_c$, the deviation in thermal expansion along c in strained PbTiO_3 compared to bulk. Figures 3 and 4 show $\Delta\alpha_c$ and its various contributions for PbTiO_3 thin-films under compressive and tensile strain for two different substrate thermal expansion coefficients (the same as those considered in Figure 2). Both figures appear to show that linear elasticity (the first term of Equation 13) makes the dominant contribution to $\Delta\alpha_c$, with the red squares almost overlaid on the black squares. In this scenario, the thermal expansion of the c -axis as a function of temperature is controlled by Poisson-like linear elastic coupling between the a and c -axes. If we were to consider *only* the linear elastic contribution to $\Delta\alpha_c$, the PbTiO_3 films would appear highly harmonic.

However, Figures 3 and 4 additionally show that there are also large contributions to $\Delta\alpha_c$ from elastic anharmonicity and anharmonic thermal stress – in the case of the PbTiO_3 thin-film under compressive strain and $\alpha_a = 2.5 \times 10^{-5}$, these terms are actually larger in magnitude than the linear elastic contribution through nearly the entire temperature range. Critically, the contributions to $\Delta\alpha_c$ from elastic anharmonicity and anharmonic thermal stress are of *opposite sign*, leading to a fortuitous near-cancellation (whereas the sign of the contribution from elastic anharmonicity is always opposite that of the anharmonic thermal stress, which one is positive and which negative depends on the sign of the misfit strain at a given temperature; for elastic anharmonicity the contribution tends to be the same sign as the misfit strain). This fortuitous near-cancellation between different types

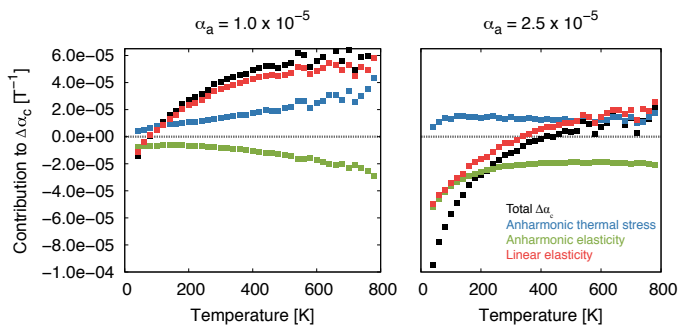


FIG. 3. Contributions to $\Delta\alpha_c$, broken down according to Equation 13, as a function of temperature for compressively strained films. The misfit strain at 300 K (ϵ_a^{300}) is -0.75% while the strain rate is varied from that of bulk PbTiO_3 . The linear elasticity contribution refers to the first term of Equation 13, the anharmonic elasticity contribution refers to the second and third terms of Equation 13 (grouped in parentheses), and the anharmonic thermal stress contribution refers to the fourth term of Equation 13.

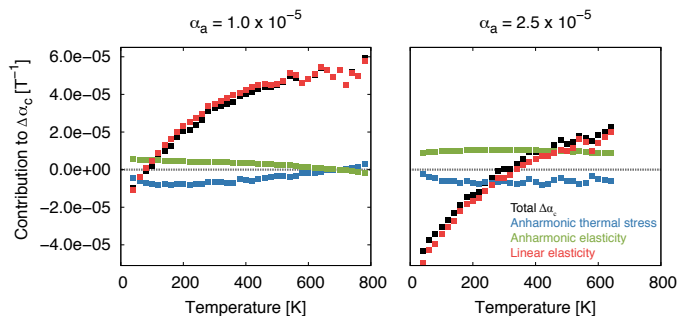


FIG. 4. Contributions to $\Delta\alpha_c$, broken down according to Equation 13, as a function of temperature for tensile strained films. The misfit strain at 300 K (ϵ_a^{300}) is $+0.75\%$, while the strain rate is varied from that of bulk PbTiO_3 . The linear elasticity contribution refers to the first term of Equation 13, the anharmonic elasticity contribution refers to the second and third terms of Equation 13 (grouped in parentheses), and the anharmonic thermal stress contribution refers to the fourth term of Equation 13.

of anharmonicity, the origin of which will be discussed in the next section, results in what looks like a linear elastic thermal response of strained PbTiO_3 thin-films.

B. Dependence of elastic constants and Grüneisen parameters on temperature and misfit strain

The near-cancellation of contributions from anharmonicity shown in Figures 3 and 4 can ultimately be attributed to changes in the elastic constants and Grüneisen parameters with temperature and misfit strain. Figure 5 shows that C_{31} , C_{33} and γ_c for the strained films can all differ significantly from bulk

PbTiO_3 , and also change significantly with temperature depending on the misfit strain and substrate thermal expansion coefficient. Despite the fact that contributions to $\Delta\alpha_c$ from just the linear elasticity term of Equation 13 closely match those calculated using the full expression for $\Delta\alpha_c$, the large strain dependencies depicted in Figure 5 corroborate the data shown in Figures 3 and 4 in illustrating that strained PbTiO_3 thin-films are highly anharmonic, especially with respect to the elastic constants (note that even though the values of γ_c tend to be fairly small, they still experience large *changes* with strain, indicating the presence of anharmonicity). The details of how the elastic constants and Grüneisen parameters change with temperature affect how elastic anharmonicity and anharmonic thermal stress contribute to changes in the c -axis of strained PbTiO_3 films with temperature.

Considering first the compressively strained film, C_{33} is softer than in bulk PbTiO_3 ($\Delta C_{33} < 0$), whereas C_{31} is stiffer ($\Delta C_{31} > 0$). The effect of these strain-induced changes to elasticity, which is captured by the second term (grouped in square brackets) in Equation 13 and the green squares in Figure 3, is to make a negative contribution to $\Delta\alpha_c$. Films under tensile strain exhibit the opposite behavior of the elastic constants compared to bulk – under tensile strain, elastic anharmonicity makes a positive contribution to $\Delta\alpha_c$, as shown by the green squares in Figure 4. The Supplementary Information contains a short discussion of how the observed effect of changes in the elastic constants on $\Delta\alpha_c$ can be predicted from a careful analysis of the sign of each of the two terms contributing to anharmonic elasticity in Equation 13.

With respect to the Grüneisen parameters, Figure 5 shows that γ_c is larger in the compressively strained film than in bulk PbTiO_3 ($\Delta\gamma_c > 0$), whereas it is smaller in the tensile strained film ($\Delta\gamma_c < 0$). Referring back to Equation 13, compressive strain then causes the anharmonic thermal stress (last) term of Equation 13 to make a positive contribution to $\Delta\alpha_c$, as shown by the blue squares in Figure 3. In contrast, the anharmonic thermal stress makes a negative contribution to $\Delta\alpha_c$ in films under tensile strain, as shown by the blue squares in Figure 4 (note that while C_{33} appears in the denominator of this term, it cannot change the sign of the term). In other words, the contribution from anharmonic thermal stress to thermal expansion along c will be the same sign as $\Delta\gamma_c$, which is typically opposite in sign to the misfit strain. The changes in contributions from the anharmonic thermal stress with respect to misfit strain are opposite those of anharmonic elasticity, as discussed above.

Hence, when PbTiO_3 undergoes biaxial strain, there is a competition between elastic anharmonicity (the second and third terms of Equation 13), and anharmonic thermal stress (the last term of Equation 13), and a large portion of their sum cancels. This near-cancellation is the result of large, simultaneous changes in elastic and vibrational properties in the film, and causes the response to appear nearly elastic, with a small departure from linear

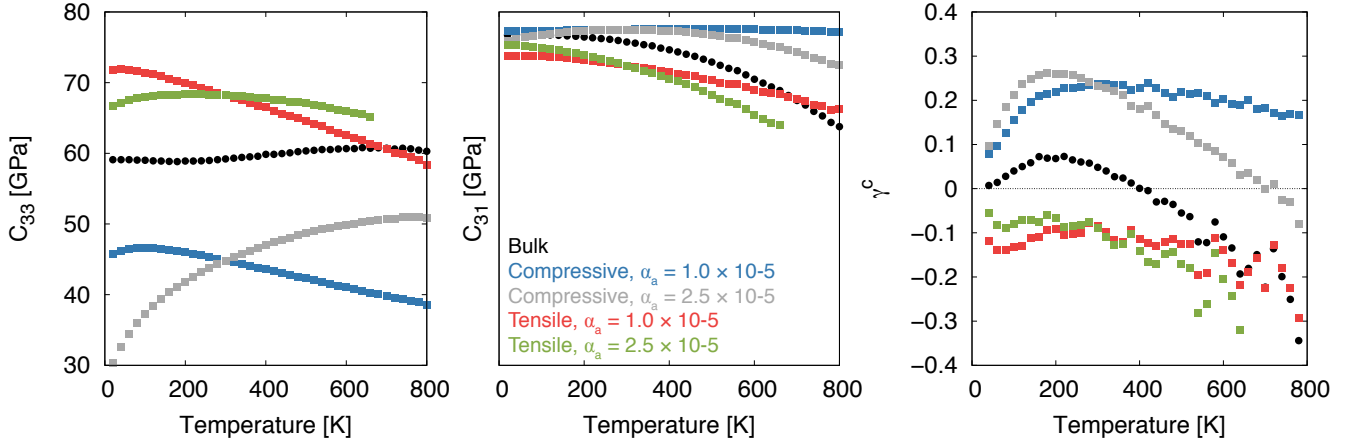


FIG. 5. Comparison between strained films on substrates with two different thermal expansion coefficients ($\alpha_a = 1.0 \times 10^{-5}$ and $\alpha_a = 2.5 \times 10^{-5}$) and bulk PbTiO₃ for C_{33} (left), C_{31} (middle) and γ_c (right) from our first-principles calculations.

elasticity due to the cancellation not being exact. The contribution to α_c from anharmonic elasticity is proportional to ΔC_{33} , which is typically the same sign as the misfit strain, and opposes the contribution from anharmonic thermal stress proportional to $\Delta\gamma_c$, which is typically the opposite sign of the misfit strain.

C. Understanding differences among strained films in terms of contributions to $\Delta\alpha_c$

Finally, returning now to Figure 2, although all of the strained films we studied exhibit suppressed negative thermal expansion along the c -axis compared to bulk (except at low temperatures for the $\alpha_a = 2.5 \times 10^{-5}$ substrate), there are differences in thermal expansion among the strained films, as noted earlier. If the behavior of the PbTiO₃ thin-films really was fully controlled by linear elasticity, the thermal expansion of the c -axis would be completely determined by the substrate thermal expansion coefficient α_a and the elastic properties of bulk PbTiO₃. Hence, the c -axis thermal expansion would be the same, regardless of the misfit strain. Instead, the details of the thermal expansion of the films do depend on both the misfit strain and the mismatch between the thermal expansion coefficients of the substrate and bulk PbTiO₃ ($\Delta\alpha_a$, the misfit strain *rate*).

For example, compressively strained films on substrates with $\alpha_a = 1 \times 10^{-5}$ show the *least* negative rate of thermal expansion along the c -axis but when α_a increases to 2.5×10^{-5} , they show the *most* negative thermal expansion along c among the thin-film systems. This is because for compressive strain and $\alpha_a = 1 \times 10^{-5}$, the positive contributions to $\Delta\alpha_c$ from anharmonic thermal stress are larger in magnitude than the negative contributions from anharmonic elasticity, pushing the thermal expansion of the c -axis to be slightly more positive than for the other strained systems, as shown in the left panel

of Figure 3. When $\alpha_a = 2.5 \times 10^{-5}$, the negative contributions to $\Delta\alpha_c$ from elastic anharmonicity are larger in magnitude than the positive contributions from anharmonic thermal stress, pushing the thermal expansion of c to be slightly more negative than for the other strained systems, as shown in the right panel of Figure 3. These trends are reversed for films under tensile strain.

Figures 3 and 4 show that, for a given strain (compressive or tensile), the anharmonic thermal stress is relatively insensitive to α_a . In addition, Equation 13 shows that neither α_a nor $\Delta\alpha_a$ appear in the (fourth) anharmonic stress term. This directs our attention to the two terms associated with anharmonic elasticity. Figure 6 shows how the average values of the two contributions to $\Delta\alpha_c$ from anharmonic elasticity terms in Equation 13 change as a function of α_a for both compressive and tensile strain. For films under compressive strain, it is the first term, $\left(2 \frac{C_{31}^{\text{bulk}}}{C_{33}^{\text{bulk}}} \Delta\alpha_a - \alpha_c^{\text{bulk}}\right) \Delta C_{33} / (C_{33}^{\text{bulk}} + \Delta C_{33})$, that has the most negative contribution to $\Delta\alpha_c$ and the most negative slope with respect to α_a . This means that for compressively strained films, it is this term that makes the contribution of elastic anharmonicity to $\Delta\alpha_c$ negative and larger in magnitude than the positive contribution from anharmonic thermal stress. Although the compressively strained film initially shows the least negative rate of thermal expansion along the c -axis among the strained films, as α_a increases the magnitude of the negative contribution from elastic anharmonicity also increases, leading the compressively strained film to exhibit the most negative rate of thermal expansion along c when $\alpha_a = 2.5 \times 10^{-5}$. For films under tensile strain, both anharmonic elastic terms are positive and increase as α_a increases – the first term again exhibits the largest contribution and slope with respect to α_a , yet this time both are positive. Hence, in this case the positive contributions to $\Delta\alpha_c$ from anharmonic elasticity grow larger in magnitude than the negative contributions from anharmonic thermal stress as α_a increases, leading to films

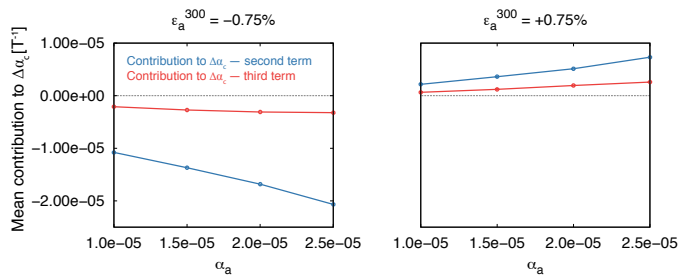


FIG. 6. Variation in contribution to $\Delta\alpha_c$ of anharmonic elasticity term of Equation 13 in terms of the second term of Equation 13 (blue) and the third term of Equation 13 (red). Data are shown as a function of substrate thermal expansion coefficient (α_a) for compressively strained ($\epsilon_a^{300} = -0.75\%$) and tensile strained ($\epsilon_a^{300} = +0.75\%$) films. Each data point corresponds to the average value of the indicated term from 0 K to 800 K. The lines are guides for the eye.

under tensile strain having a slower rate of thermal expansion along the c -axis than either bulk PbTiO_3 or compressively strained films. As discussed in Section IV B and the Supplementary Information, the sign of this critical first term is determined by the sign of ΔC_{33} , which is the same as the sign of ϵ_a . The behavior of this term, combined with the relative insensitivity of anharmonic thermal stress on α_a , explains the departure of $\Delta\alpha_c$ from what would be predicted by linear elasticity alone.

D. Explaining thermal expansion in experimentally synthesized PbTiO_3 thin-films

We can use our findings above to explain the experimentally observed thermal expansion behavior of PbTiO_3 thin-films on LSAT,[32] SrTiO_3 [33] and DyScO_3 [34] substrates. Figure 7 shows the lattice parameters and thermal expansion coefficients as functions of temperature for PbTiO_3 thin-films on all three substrates. All three substrates have similar thermal expansion coefficients – from 0 – 800 K, α_a is fairly low and constant with temperature with average values of $0.93 \times 10^{-5} \text{ K}^{-1}$, $1.10 \times 10^{-5} \text{ K}^{-1}$, and $1.04 \times 10^{-5} \text{ K}^{-1}$, for LSAT, SrTiO_3 , and DyScO_3 , respectively. In each case the thermal expansion along c is less negative than in bulk PbTiO_3 , however the α_c for each substrate is different, and the framework established in this study explains why.

At 300 K, LSAT induces a large compressive misfit strain of -1.01%, SrTiO_3 a small strain of -0.01%, and DyScO_3 induces a large tensile strain of +1.01%. We showed above that under compressive strain and when α_a is small, the negative magnitude of the contribution to $\Delta\alpha_c$ from elastic anharmonicity is smaller than the positive contribution from anharmonic thermal stress, leading to a smaller rate of negative thermal expansion along c compared to both bulk and tensile strained films. By this reasoning, PbTiO_3 on LSAT should show the

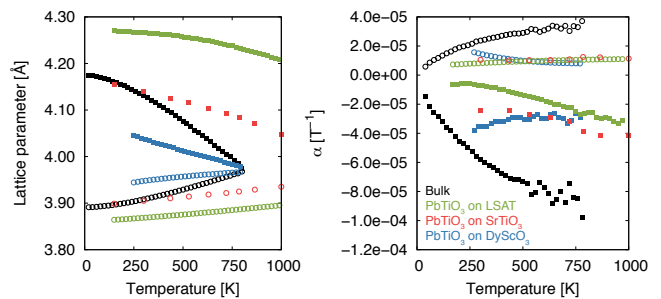


FIG. 7. Comparison between lattice parameters (left) and thermal expansion coefficients (right) of bulk PbTiO_3 and strained PbTiO_3 thin-films on LSAT, DyScO_3 and SrTiO_3 substrates. Substantially similar data are reported in Ref. 21, however in this work we used a slightly more dense grid for our QHA calculations. Open circles denote data for the a -axis lattice parameters and α_a (experimental data for SrTiO_3 , DyScO_3 , and LSAT[32–34]), whereas closed squares denote data for the c -axis lattice parameters and α_c (predicted from our QHA calculations).

least negative thermal expansion along c and PbTiO_3 on DyScO_3 should show the most negative thermal expansion along c ; this is indeed what is shown in Figure 7. Put another way, we showed earlier that the sign of the contribution from anharmonic thermal stress to $\Delta\alpha_c$ has the opposite sign of the misfit strain. Therefore, we would expect $\Delta\alpha_c$ to be most positive in LSAT and most negative in DyScO_3 , and this is indeed what we see.

V. SUMMARY AND CONCLUSIONS

Our results reveal that although PbTiO_3 thin-films are highly anharmonic, a fortuitous near-cancellation between the thermal stress and anharmonic elastic contributions to the temperature-dependent structural parameters means that the thermal response of the c -axis of the films can be predicted very well using only the misfit strain and bulk PbTiO_3 properties. We note that the $\Delta\gamma^c$ term, which contributes to the anharmonic thermal stress, involves the *derivative* of the Grüneisen parameter with respect to strain. Since the Grüneisen parameter is a function of the third-order interatomic force constants (and higher order, if sublattice displacements are present, as is the case for ferroelectric PbTiO_3 [23, 24]), $\Delta\gamma^c$ is a function of the *fourth* and higher-order force constants. Additionally, as elastic constants are related to the curvature of the Helmholtz free energy surface, the large changes in the elastic constants with strain are also driven by changes in both electronic and vibrational free energy, and thus the third, fourth, and higher-order force constants [35]. The low thermal conductivity observed for bulk PbTiO_3 [36, 37] corroborates these findings. In this light however, the approximately linear-elastic behavior of the strained PbTiO_3 thin-films is unexpected.

Our findings may also help explain why popular phe-

nomenological models for predicting the strain behavior of the polarization in ferroelectric PbTiO₃ thin-films, such as those described in Refs. 38 and 39, are reasonably effective at capturing the thermal expansion behavior of both bulk and epitaxially strained films of PbTiO₃ with temperature [40–43], despite being functions of the elastic constants of the high-symmetry cubic phase, and with no explicit elastic anharmonicity included beyond its coupling to the polarization. If the structural behavior of ferroelectric PbTiO₃ films clamped to a substrate can be well-described by linear elasticity with much of the higher-order anharmonicity ignored, it stands to reason that the inclusion of higher-order elastic coupling terms beyond the few judiciously chosen in the above models would be unnecessary to accurately capture the structural evolution of the system with temperature.

Finally, our work shows that the thermal expansion behavior of PbTiO₃ films depends on the misfit strain throughout the *entire* temperature range. This means it depends on not only the misfit strain between film and substrate lattice parameters at a single temperature, but on the misfit between their thermal strain *rates*, which determines how misfit strain accumulates with tempera-

ture. These dependencies are entwined in a complex way – the misfit strain between the lattice parameters of the substrate and the equilibrium (bulk) lattice parameters of the film material can induce large changes in the elastic properties and Grüneisen parameters of the film, which themselves influence how the *c*-axis of the film responds to the misfit strain rate. Our combined first-principles and phenomenological approach provides significant insights into this behavior and offers a systematic framework for exploring thermal expansion phenomena in both bulk and thin-film systems.

ACKNOWLEDGMENTS

This work was supported by the National Science Foundation. E. T. R. and N. A. B. were supported by DMR-1550347. Computational resources were provided by the Cornell Center for Advanced Computing and the Extreme Science and Engineering Discovery Environment (XSEDE) through allocation DMR-160052.

-
- [1] M. G. Tucker, A. L. Goodwin, M. T. Dove, D. A. Keen, S. A. Wells, and J. S. Evans, *Phys. Rev. Lett.* **95**, 255501 (2005).
 - [2] N. Mounet and N. Marzari, *Phys. Rev. B* **71**, 205214 (2005).
 - [3] D. S. Kim, O. Hellman, J. Herriman, H. Smith, J. Lin, N. Shulumba, J. Niedziela, C. Li, D. Abernathy, and B. Fultz, *Proc. Natl. Acad. Sci. U.S.A.* **115**, 1992 (2018).
 - [4] E. T. Ritz and N. A. Benedek, *Phys. Rev. Lett.* **121**, 255901 (2018).
 - [5] A. L. Goodwin, D. A. Keen, and M. G. Tucker, *Proc. Natl. Acad. Sci. U.S.A.* **105**, 18708 (2008).
 - [6] A. L. Goodwin, D. A. Keen, M. G. Tucker, M. T. Dove, L. Peters, and J. S. O. Evans, *J. Am. Chem. Soc.* **130**, 9660 (2008).
 - [7] A. L. Goodwin, B. J. Kennedy, and C. J. Kepert, *J. Am. Chem. Soc.* **131**, 6334 (2009).
 - [8] C. Lind, *Materials* **5**, 1125 (2012).
 - [9] W. Miller, C. Smith, D. Mackenzie, and K. Evans, *J. Mater. Sci.* **44**, 5441 (2009).
 - [10] G. D. Barrera, J. A. O. Bruno, T. H. K. Barron, and N. L. Allan, *J. Phys. Condens. Matter* **17**, R217 (2005).
 - [11] I. Yanase, T. Kojima, and H. Kobayashi, *Solid State Commun.* **151**, 595 (2011).
 - [12] C. Ablitt, H. McCay, S. Craddock, L. Cooper, E. Reynolds, A. A. Mostofi, N. C. Bristowe, C. A. Murray, and M. S. Senn, *Chem. Mater.* (2019).
 - [13] J. Chen, X. Xing, R. Yu, and G. Liu, *J. Am. Ceram. Soc.* **88**, 1356 (2005).
 - [14] G. Shirane and S. Hoshino, *J. Phys. Soc. Jpn.* **6**, 265 (1951).
 - [15] P.-E. Janolin, F. Le Marrec, J. Chevreul, and B. Dkhil, *Appl. Phys. Lett.* **90**, 192910 (2007).
 - [16] P.-E. Janolin, *Journal of Materials Science* **44**, 5025 (2009).
 - [17] P. Giannozzi, S. Baroni, N. Bonini, M. Calandra, R. Car, C. Cavazzoni, D. Ceresoli, G. L. Chiarotti, M. Cococcioni, I. Dabo, *et al.*, *J. Phys. Condens. Matter* **21**, 395502 (2009).
 - [18] Z. Wu and R. E. Cohen, *Phys. Rev. B* **73**, 235116 (2006).
 - [19] K. F. Garrity, J. W. Bennett, K. M. Rabe, and D. Vanderbilt, *Comput. Mater. Sci.* **81**, 446 (2014).
 - [20] E. T. Ritz, S. J. Li, and N. A. Benedek, *J. Appl. Phys.* **126**, 171102 (2019).
 - [21] E. T. Ritz and N. A. Benedek, *Physical Review Materials* **4**, 084410 (2020).
 - [22] Our DFT simulations predict that the unit cell of bulk PbTiO₃ exhibits unstable phonon modes at 0 K in its cubic phase, as well as for nearly-cubic unit cells with very low *c/a* ratios. This results in difficulty when calculating QHA grid points very close to the tetragonal-cubic phase transition. The lowest value of *c* in the set of unit cells used in our quasiharmonic grid is approximately 4.00 Å, meaning that for temperatures greater than 720 K, the point that minimizes the Helmholtz free energy surface fit is no longer bounded by that grid along the *c* axis. While such an extrapolation of the derivatives of the vibrational free energy is within the spirit of the Grüneisen theory of thermal expansion, our simulation can be interpreted to conclude that the tetragonal-cubic phase transition occurs somewhere within the range of 720 K to 800 K.
 - [23] D. C. Wallace, *Thermodynamics of Crystals* (Wiley, 1972).
 - [24] G. K. Horton and A. A. Maradudin, *Dynamical Properties of Solids*, Vol. 1 (Elsevier, 1974).
 - [25] C. Choy, S. Wong, and K. Young, *Phys. Rev. B* **29**, 1741 (1984).
 - [26] N. W. Ashcroft and N. D. Mermin, *Solid State Physics*

- (Holt, Rinehart and Winston, New York, 1976).
- [27] R. Munn, *J. Phys. C: Solid State Physics* **5**, 535 (1972).
 - [28] T. Barron and M. Klein, *Proceedings of the Physical Society (1958-1967)* **85**, 523 (1965).
 - [29] D. C. Wallace, *Reviews of Modern Physics* **37**, 57 (1965).
 - [30] H. Wang and M. Li, *Physical Review B* **85**, 104103 (2012).
 - [31] The films under compressive and tensile strain at 300 K remain under compressive and tensile strain throughout nearly the entire temperature range studied (the only exception is the film constrained by the substrate with $\varepsilon_a^{300} = +0.75\%$ at $\alpha_a = 1 \times 10^{-5}$ for temperatures over 700 K).
 - [32] B. Chakoumakos, D. Schlom, M. Urbanik, and J. Luine, *J. Appl. Phys.* **83**, 1979 (1998).
 - [33] D. de Ligny and P. Richet, *Phys. Rev. B* **53**, 3013 (1996).
 - [34] M. Biegalski, J. Haeni, S. Trolier-McKinstry, D. Schlom, C. Brandle, and A. V. Graitis, *J. Mater. Res.* **20**, 952 (2005).
 - [35] D. Dangić, A. R. Murphy, É. D. Murray, S. Fahy, and I. Savić, *Physical Review B* **97**, 224106 (2018).
 - [36] M. Tachibana, T. Kolodiazhnyi, and E. Takayama-Muromachi, *Applied Physics Letters* **93**, 092902 (2008).
 - [37] I. Yoshida, *Journal of the Physical Society of Japan* **15**, 2211 (1960).
 - [38] N. Pertsev, A. Zembilgotov, and A. Tagantsev, *Phys. Rev. Lett.* **80**, 1988 (1998).
 - [39] A. G. Zembilgotov, N. A. Pertsev, H. Kohlstedt, and R. Waser, *Journal of Applied Physics* **91**, 2247 (2002), cond-mat/0111218.
 - [40] M. Highland, D. Fong, G. Stephenson, T. Fister, P. Fuoss, S. Streiffer, C. Thompson, M.-I. Richard, and J. Eastman, *Appl. Phys. Lett.* **104**, 132901 (2014).
 - [41] C. Lichtensteiger, J.-M. Triscone, J. Junquera, and P. Ghosez, *Physical review letters* **94**, 047603 (2005).
 - [42] S. Venkatesan, A. Vlooswijk, B. J. Kooi, A. Morelli, G. Palasantzas, J. T. De Hosson, and B. Noheda, *Phys. Rev. B* **78**, 104112 (2008).
 - [43] M. J. Haun, E. Furman, S. Jang, H. McKinstry, and L. Cross, *J. Appl. Phys.* **62**, 3331 (1987).